

Importance of chirality and reduced flexibility of protein side chains: A study with square and tetrahedral lattice models

Jinfeng Zhang¹, Yu Chen², Rong Chen^{1,2,3}, and Jie Liang¹ *
¹*Departments of Bioengineering and* ²*Information & Decision Science*
University of Illinois at Chicago
845 S. Morgan St, Chicago, IL 60607
³*Department of Business Statistics & Econometrics*

Peking University
Beijing, P.R. China

(Accepted by *J. Chem. Phys.*)

(Dated: October 24, 2018)

Side chains of amino acid residues are the determining factor that distinguish proteins from other unstable chain polymers. In simple models they are often represented implicitly (*e.g.*, by spin-states) or simplified as one atom. Here we study side chain effects using two-dimensional square lattice and three-dimensional tetrahedral lattice models, with explicitly constructed side chains formed by two atoms of different chirality and flexibility. We distinguish effects due to chirality and effects due to side chain flexibilities, since residues in proteins are *L*-residues, and their side chains adopt different rotameric states. For short chains, we enumerate exhaustively all possible conformations. For long chains, we sample effectively rare events such as compact conformations and obtain complete pictures of ensemble properties of conformations of these models at all compactness region. This is made possible by using sequential Monte Carlo techniques based on chain growth method. Our results show that both chirality and reduced side chain flexibility lower the folding entropy significantly for globally compact conformations, suggesting that they are important properties of residues to ensure fast folding and stable native structure. This corresponds well with our finding that natural amino acid residues have reduced effective flexibility, as evidenced by statistical analysis of rotamer libraries and side chain rotatable bonds. We further develop a method calculating the exact side-chain entropy for a given back bone structure. We show that simple rotamer counting underestimates side chain entropy significantly for both extended and near maximally compact conformations. We find that side chain entropy does not always correlate well with main chain packing. With explicit side chains, extended backbones does not have the largest side chain entropy. Among compact backbones with maximum side chain entropy, helical structures emerges as the dominating configurations. Our results suggest that side chain entropy may be an important factor contributing to the formation of alpha helices for compact conformations.

Keywords: chirality, flexibility, packing, side chain entropy, sequential Monte Carlo.

I. INTRODUCTION

Side chains of amino acid residues are the determining factor that distinguish proteins from other unstable chain polymers. Their arrangement along primary sequence dictates the native structure of proteins. Side chains are also responsible for much of the complexity of protein structure^{1,2,3,4,5}. They pack tightly, but also leave space to form voids and pockets^{6,7,8}. The effects of simplified side chain were studied in details for two dimensional square lattice and three dimensional cubic lattice models in

reference¹. Such studies of simplified models played important roles in elucidating the principles of protein folding⁹, because these models allow enumeration of all feasible conformations and calculation of exact entropy for short chain molecules. They are also amenable to detailed sampling for longer chain models. However, the effects of side chains are still not fully understood. Several studies on side chain effects rely on implicit models or assign different spin states to each monomer to mimic the internal degrees of freedom of side chains^{10,11}. It is not clear how realistic these model are without explicit side chains. In studies where side chains are modeled explicitly, they are simplified: only one atom is attached to the main chain monomer¹. Since there is no internal degree of freedom for side chains of one atom, χ -angles and rotamirc states of side chains¹²

*Corresponding author. Phone: (312)355-1789, fax: (312)996-5921, email: jliang@uic.edu

cannot be studied.

In this study, we introduce more realistic side chain models. We make the distinction of two different side chain effects that have not been investigated previously. We first study the chirality effects. Chirality effects at C_α atom of a residue arises because the four atoms bonded with C_α are different¹³. Side chain atom C_β can be attached to different positions of C_α relative to other atoms (C , N , and H atoms). In Nature, all amino acid residues with side chains are of the L configuration instead of the D configuration, *i.e.*, the position of C_β in relationship to C and N atoms are all in a unique chiral state. The origin of this bias is unclear and remains a puzzle in the studies of the origin of life^{14,15}. We also study the flexibility effects. Flexibility effects arise because additional atoms beyond C_β can rotate around a single side chain chemical bond, regardless of the chiral state of C_α ^{16,17}. These two effects are different: There is a large energetic barrier for change of chiral state, which often involves the breaking of a chemical bond. In contrast, rotation along a single bond is relatively easy.

We use lattice models to study the effects of both chirality and flexibility. We introduce chirality models for two-dimensional square lattice and three-dimensional tetrahedral lattice polymers. To model side chain flexibility, we use explicitly side chains consisting of two atoms, which enable the modeling of rotational degree of freedom of side chains. Because this leads to significant increases of the size of conformational space, it is difficult to characterize accurately ensemble properties of compact conformations of polymers. We use the techniques of sequential Monte Carlo importance sampling and resampling to generate properly weighted samples of rare events, such as long chain conformations with maximum compactness.

We examine the distribution of all geometrically feasible conformations of self-avoiding walks on lattice with side chains of different chirality and flexibility. We focus on their packing properties and their conformational entropy. Folding into a well defined native structure is accompanied with large reduction in conformational entropy. We explore how entropy of folding is affected by chirality and flexibility, and how it relates to the compactness of chain polymers with side chains. Because the absolute number of compact conformation changes dramatically after incorporation of chirality and side chain flexibility, it is not obvious whether these factors helps or hinders protein folding. Our results indicate that chiral molecules have lower entropy of folding than achiral

models. Models with less side chain flexibility also have significant lower entropy of folding than models with more flexible side chain.

Side chain entropy is important for protein folding and its estimation is the subject of several studies^{1,18,19,20,21}. To calculate side chain entropy precisely for our model polymers, we introduce an algorithm for counting the exact number of side chain conformations. It is based on the observation of disconnected sets in the conflict graph of side chain correlations. In comparison, we find rotamer counting²² significantly overestimates side chain entropy, and the difference is more pronounced in most extended as well as in protein-like near compact regions of main chain structures.

In addition, we revisit two models of protein packing, namely, the jigsaw puzzle model and the nuts and bolts model. We show that packing of chain polymers with chiral side chains included is more like nuts and bolts than jigsaw puzzles.

The results presented here are in agreement with the chiral nature of L-amino acid residues found in natural proteins and an analysis of flexibility of residues in real proteins. They suggest that both chirality and restriction in flexibility make important contributions to protein folding. Our presentation is organized as follows: We first introduce side chain models for chirality and flexibility effects in two-dimensional square lattice and three-dimensional tetrahedral lattice. This is followed by a description of the parameters used in our study and the algorithm for counting side chain conformations. The results of chirality and flexibility on conformational entropy by enumeration and by sequential Monte Carlo sampling are then presented. We then compare rotamer counting and the exact method developed here for calculating side chain conformational entropy. We conclude with remarks and discussion.

II. MODELS AND METHODS

a. Lattice side chain models. For two-dimensional square lattice and three-dimensional tetrahedral lattice models, a side chain consists of one or two *atoms* attached to each main chain *monomer*. There are no side chains for the two terminal monomers following reference¹ (Figure 1). For three-dimensional models, we use tetrahedral lattice instead of cubic lattice. The coordination and bond connection of a tetrahedral unit are very

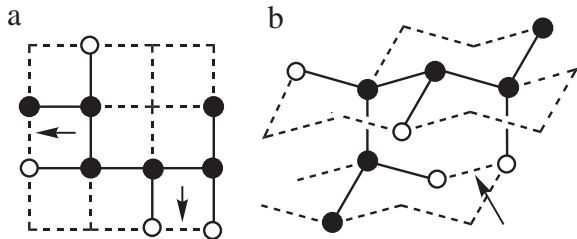


FIG. 1: Lattice side chain models of 6-mers (a) on square lattice with side chain of size one and (b) on tetrahedral lattice with side chain of size one. Filled circles represent main chain monomers and empty circles represent side chain atoms. In these examples, side chains have one atom. Arrows pointing to spatial contacts between non-bonded atoms.

similar to carbon atoms with four chemical bonds, which is the most abundant element in proteins. Both chirality and flexibility can be modeled effectively using tetrahedral lattice. In addition, tetrahedral lattice has the advantage that real protein structures can be well approximated^{23,24}.

b. Models for chirality. A molecule that is distinct from its mirror image is a chiral molecule. The idea of “chirality” in molecule goes back to Pasteur, who observed in 1848 that crystals of tartaric acid rotated polarized light in different directions, either to the right (D for “*dextro*”) or left (L for “*levo*”)²⁵. Here we consider chirality due to different attachments of non-identical atoms to the C_α atom.

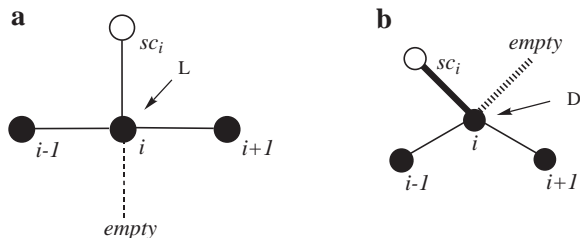


FIG. 2: Assignment of chirality for models in planar square lattice and three dimensional tetrahedral lattice. (a) A two-dimensional L -residue in square lattice. From the backbone monomer (filled circle) of residue $i + 1$ to the side chain atom (sc_i , empty circle) of residue i , then to the empty site, we turn counter clockwise. (b). A three-dimensional D residue in tetrahedral lattice. Taking the view point along the vector pointing from the backbone monomer of residue i to the empty site, the backbone atoms of residues $i + 1$, $i - 1$, and the side chain atom (sc_i) of residue i are arranged in a clockwise fashion.

We first introduce chirality for two-dimensional lattice model. Planar chirality arises if a two-dimensional molecule and its reflection (mirror image about a line) cannot be superimposed. For a chiral residue, the placement of side chain atoms is restricted. The chirality of a residue i is determined by the relative orientation of its attached side chain atom and the preceding and succeeding main chain monomers of residues $i - 1$, $i + 1$ (Figure 2a). For a chiral residue i , if we start from the main chain monomer of the succeeding residue $i + 1$ and go through the side chain atom of residue i (sc_i) to the unoccupied site (unoccupied by the two backbone monomers of residues $i - 1$, $i + 1$, and side chain sc_i), the chirality of residue i is L if we turn counter clockwise, and D if we turn clockwise.

For three dimensional tetrahedral lattice, chirality of a residue can be defined realistically following that of the C_α in amino acids (Figure 2b). We take a view point along the vector pointing from the backbone monomer of i to the empty site unoccupied by backbone monomers of residues $i - 1$, $i + 1$, and side chain atom of residue i . If the backbone monomers $i + 1$, $i - 1$, and the side chain of residue i are arranged counter clockwise, the chirality of residue i is L . If they are arranged clockwise, the chirality is D . For achiral models in both square lattice and tetrahedral lattice, there is no restriction for the allowed positions for the first side chain atom and it can take any of the two available sites unoccupied by backbone monomers of $i - 1$, i , and $i + 1$ -th residues.

We study both chiral molecules and achiral molecules in this work. In a chiral molecule, the first atom of all side chains follow strictly one fixed chirality (either D or L, we use D for this study). In an achiral molecule, there is no restriction and the first atom of a side chain can take any unoccupied reachable site.

c. Models for side chain flexibility. Regardless whether a residue is chiral or achiral, it is possible to have a flexible side chain if the side chain consists of two or more atoms. Because square lattice and tetrahedral lattice both have coordination number of four, there are at most three possible sites available when attaching a new side chain atom. This models well the χ_1 angles of protein side chains, as they often can be grouped into mainly three clusters: t , g^+ , and g^- , which stand for trans, gauche positive, and gauche negative, respectively²⁶. Depending on whether any of these sites are forbidden, a side chain atom in tetrahedral lattice may have 1, 2, or 3 allowed positions (Figure 3). In model M_1 , the second side chain atom can only be placed at

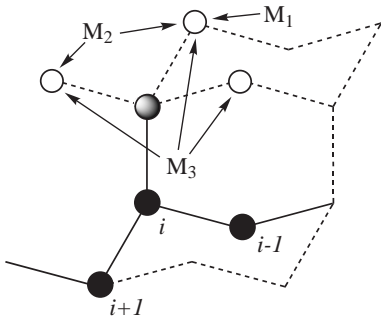


FIG. 3: Rotameric positions of M_1 , M_2 , and M_3 side chain flexibility model. Facing the vector pointing from backbone atom i to its first side chain atom, M_1 position for the second side chain atom is located in the opposite direction to the vector connecting backbone atom i to backbone atom $i + 1$. M_2 model contains an additional site for the second side chain atom, which is located in the opposite direction to the vector connecting backbone atom i to backbone atom $i - 1$. For M_3 model, the second side chain atom can occupy any of the three reachable sites.

one fixed position. In model M_2 , the second side chain atom can be placed at one additional possible position, and in model M_3 , the second side chain atom can be placed at any of the three possible positions. Facing the vector pointing from backbone atom i to its first side chain atom, M_1 position for the second side chain atom is located in the opposite direction to the vector connecting backbone atom i to backbone atom $i + 1$. M_2 model contains an additional site for the second side chain atom, which is the immediate neighbor of M_1 in counterclockwise direction. For M_3 model, the second side chain atom can occupy any of the three reachable sites.

d. Contact and Compactness. We focus on protein-like compact conformations. Two non-bonded monomer (backbone or side chain) n_i and n_j are in topological contact if they are spatial neighbors. Two main chain monomers are in contact only if they are not sequential neighbor ($i \neq j \pm 1$, see arrows in Figure 1).

The parameter measuring compactness ρ of a conformation is defined as the ratio between its number of topological contacts and the maximum number of contact attainable for a particular sequence of given chain length²⁷:

$$\rho \equiv \frac{t}{t_{max}}, \quad \text{where } 0 \leq \rho \leq 1.$$

e. Entropy and excess entropy. We are interested in the effects of different models of side chain chirality and flexibility on the conformational space

of chain polymers. We study only homopolymers and do not investigate the relationship between sequence and conformation.

Since homopolymers do not fold into a unique stable ground state conformation, we calculate the entropy for homopolymers to adopt conformations at a specific compactness value ρ . We define entropy $S(\rho)$ for conformations with compactness ρ as:

$$S(\rho) = k_B \ln n(\rho),$$

where k_B is the Boltzmann constant, $n(\rho)$ is the number of conformations with compactness ρ . Similarly, side chain entropy $S_{sc}(B)$ is defined for a fixed backbone conformation B as:

$$S_{sc}(B) = k_B \ln n_{sc}(B),$$

where $n_{sc}(B)$ is the number of all self-avoiding side chain arrangements for the fixed backbone conformation B . The overall entropy S for all conformations is given by:

$$S = k_B \ln \sum_i n(\rho_i) = k_B \ln \sum_j n_{sc}(B_j).$$

The change ΔS in the conformational entropy between folded state (F) and unfolded state (U) is given by:

$$\Delta S = S_F - S_U.$$

For lattice models used in this study, folded state is defined as conformations with compactness $\rho = \rho_{max} \equiv 1$. Unfolded states correspond to all conformations with compactness $\rho < 1$. We have:

$$\Delta S(\rho_{max}) = S(\rho_{max}) - S(\rho < 1).$$

Since conformations with ρ_{max} constitute a very small proportion among all conformations: $S(\rho < 1) \approx S$, we have:

$$\Delta S(\rho_{max}) \approx S(\rho_{max}) - S = k_B \ln \frac{n(\rho_{max})}{\sum_i n(\rho_i)} = k_B \ln \omega(\rho_{max}),$$

where $\omega(\rho_{max})$ is the fraction of maximum compact conformations. For convenience, we define folding entropy ΔS_f of the maximum compact conformations as the absolute value of the above entropy change:

$$\Delta S_f = |\Delta S(\rho_{max})| = -k_B \ln \omega(\rho_{max}).$$

We define entropic change $\Delta S(\rho)$ at other compactness as:

$$\Delta S(\rho) = |\Delta S(\rho)| = -k_B \ln \omega(\rho).$$

To compare folding entropies of models with different chirality and flexibility, we follow reference¹ and define the excess entropy $ES_{a,b}$ for model a when compared to model b as:

$$ES_{a,b} = \Delta S_f(a) - \Delta S_f(b) = -k_B \ln \frac{\omega_a(\rho_{max})}{\omega_b(\rho_{max})},$$

where $\omega_a(\rho_{max})$ and $\omega_b(\rho_{max})$ are the fractions of maximum compact conformations for model a and model b , respectively.

f. Radius of gyration R_g . Radius of gyration (R_g) is a parameter frequently used to measure the global compactness of a conformation. For a set of n atoms, R_g is the root-mean-square distance of position $\mathbf{x}_i \in \mathbb{R}^3$ of each atom i to their geometric center $\bar{\mathbf{x}} = \sum_{i=1}^n \mathbf{x}_i/n$:

$$R_g = \left(\sum_{i=1}^n (\mathbf{x}_i - \bar{\mathbf{x}})^2/n \right)^{1/2}.$$

For globular proteins, the value of R_g fluctuates but can be predicted with reasonable accuracy from the number of residues by the relationship $R_g \approx 2.2N^{1/3}$, which describes accurately globally compact proteins²⁸.

g. Sequential Monte Carlo importance sampling. In this study, we need to estimate properties of rare events, namely, properties of conformations with maximum number of contacts ρ_{max} , *e.g.*, the fraction of conformations with $\rho = \rho_{max}$. Estimating properties of rare events is difficult, because finding such conformations is challenging when more extended conformations dominate in the whole population of all geometrically feasible self-avoiding walks with side chains. We adopt the same sequential Monte Carlo strategy for sampling as that of a recent three dimensional off-lattice study, where thousands of polymers of length 2,000 at very high compactness values were successfully generated²⁹. Sequential Monte Carlo is an effective strategy based on chain growth for sampling high dimensional space^{30,31}. The details of studying lattice models using this technique have been described elsewhere^{29,32}. It was shown previously that sequential Monte Carlo can give accurate estimation of ensemble properties of lattice conformations, as verified by comparison with results obtained from exhaustive enumeration^{29,32}.

Once a sample conformation is generated, we need to find out whether it is maximally compact. For two dimensional square lattice models, the upper bound of the number of contacts t^* for polymers in which all beads (including main chain monomers and side

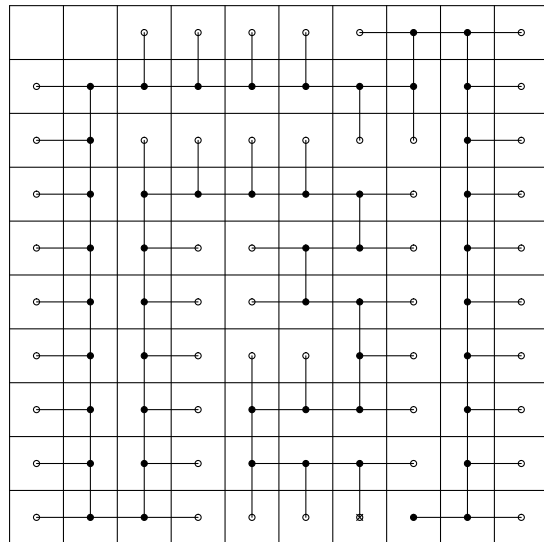


FIG. 4: A maximum compact conformation on square lattice for achiral model of side chain size one. Solid circles are backbone monomers, and empty circles are side chain atoms. The main chain length is 50.

chain atoms) are connected can be calculated. For any polymers with N beads, t^* is:

$$\begin{aligned} t^* &= N - 2m, \text{ for } m^2 < N \leq m(m+1) \\ t^* &= N - 1 - 2m, \text{ for } m(m+1) < N \leq (m+1)^2, \end{aligned} \quad (1)$$

where m is a positive integer³³. It is easy to verify that this bound is tight for polymers without side chains and gives the maximum number of contact t_{max} .

Finding the maximum number of contacts for models with side chain is more difficult, since no closed-form answers are known for various side chain models studied here. The compactness ρ is therefore difficult to calculate for long chain polymers. With the introduction of side chains, it is possible that the maximum compact conformations may not take t^* as t_{max} due to the requirement of side chain connectivity and self avoidance. For two dimensional square lattice models with side chain of size one, we find from exhaustive enumeration that there are conformations with maximum contact of t^* for chains up to length $N = 18$ in achiral model. No conformations with t^* contacts exist for chiral model. For longer chains, we generate samples of conformations using sequential Monte Carlo for length up to $N = 100$. We found that for achiral models, there

exist sampled conformations with t^* contacts at every length from 19 to 100. This suggests that it is likely that achiral models with side chain of side one have $t^* = t_{max}$ at length $N \geq 2$. It also indicates that this sampling strategy is effective and our method can give correct estimation of the maximum number of contact t_{max} and compactness ρ for two dimensional achiral model. An example of maximum compact conformation for achiral model of length 50 on square lattice obtained using sequential Monte Carlo is shown in Figure 4, with $N = 98$ and $m = 9$.

Verified successful results in two-dimensional models are helpful in assessing the effectiveness of sampling for three-dimensional models. Both tetrahedral lattice models and square lattice models have the same coordination number of four. In addition, conformations from chiral model is a subset of that of achiral model. We postulate that our method can give satisfactory estimation of ρ_{max} for tetrahedral models used in this study.

h. Exact calculation of side chain entropy. Rotamer counting is a widely used method to estimate side chain entropy of residues in proteins when the backbone structure is given²². The idea is to count available rotameric states for each monomer independently, and estimate the total number of states by multiplication. This approach would be accurate if all possible placement of side chains at different residues are independent. The problem is that not all combinations of rotameric states for residues along the main chain are self-avoiding. Hence this method inherently overestimate conformational entropy. The extent of the over-estimation and its effect in assessing protein folding entropy is unknown.

Calculating the exact number of all valid side chain conformations for a given main chain structure is challenging, since this requires explicit enumeration of all possible spatial arrangement of side chains. Here we introduce an algorithm for counting side chain conformations based on the divide-and-conquer paradigm.

For a fixed backbone structure, if the placement of side chain atoms of a residue affects the allowed positions of side-chain atoms of another residue, we say there is a conflict for side chains of these two residues. We can construct a conflict graph $G = (V, E)$, where V is the set of residues, and E is the set of edges representing conflicts between pairs of residues. All residues in a molecule can be grouped into m individual sets, each representing a disconnected component of the conflict graph G . When two sets are disconnected, side-chain place-

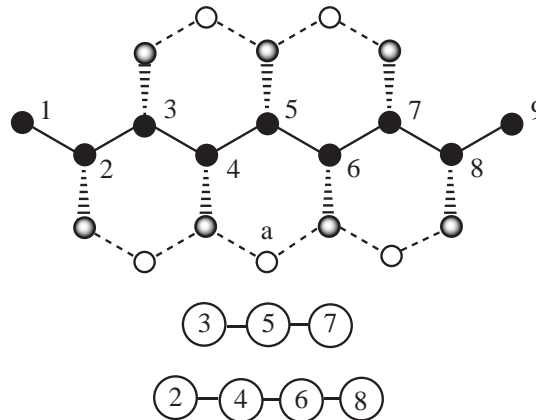


FIG. 5: An illustration of calculation of side chain entropy. (a) An extended conformation. Filled circles are main chain monomers, gray circles are first side chain atoms, and empty circles are positions that could be occupied by side chain atoms of either of two different residues. (b) The conflict graph of the conformation. There are two disconnected components in the conflict graph, one formed by residues 3, 5, and 7, and another by residues 2, 4, 6, and 8. The latter can be further divided into two smaller components by cutting at position a .

ment of residues in one set does not affect the placement of side-chains of residues in another set. The disconnected components in graph G can be identified using depth-first-search³⁴. We can then calculate the number of different side-chain arrangement n_i for each set i by enumeration. The total number N of side chain conformations of all residues is obtained by multiplication: $N = \prod_{i=1}^m n_i$. A simple example is shown in Figure 5a and Figure 5b, where a graph is constructed for an extended backbone structure. The residues can be decomposed into two independent components, one formed by residues with side chains above the main chain, and another formed by residues with side chains below the main chain.

i. Helix content on tetrahedral lattice. For a fragment of four consecutive monomers (from i to $i + 3$), there are three possible conformations on a tetrahedral lattice: left turn fragment, right turn fragment, and straight fragment (see Figure 6). For a fragment of five consecutive monomers, the 4-prefix fragment (i to $i + 3$) and the 4-suffix fragment ($i + 1$ to $i + 4$) can have any of the above three conformations. If the 4-prefix and 4-suffix fragments are of all left turns or all right turns, this five monomer fragment is defined as a helix. Helices with all left turns are defined as left-hand helices, and helices with all right turns are defined as right-hand helix.

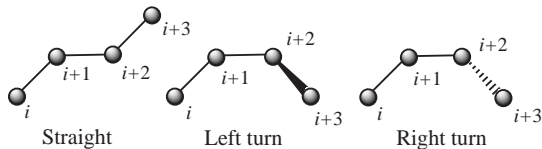


FIG. 6: The three possible conformations of a four-fragment backbone conformations.

We include both types of helices and their mixture when calculating helix content of a backbone conformation. Specifically, the helix content h of a backbone conformation of length N is:

$$h = \sum_{i=0}^{N-5} \mathbb{I}(i)/(N-4),$$

where $\mathbb{I}(i) = 1$ if the fragment of residues from i to $i+4$ is a helix by the above definition, and $\mathbb{I}(i) = 0$ otherwise.

III. RESULTS

A. Exact conformational space by enumeration

For short polymers with side chains, we obtain a complete picture of the ensemble properties of conformations by exhaustive enumeration. Table I lists the total number of conformations of different side chain models obtained from exhaustive enumeration. For longer polymers, the full conformational space cannot be enumerated, and it is necessary to use sequential Monte Carlo sampling to generate properly weighted samples from the uniform distribution of all geometrically feasible self-avoiding walks with various types of side chains.

B. Effects of side chain chirality

j. Distribution of conformations and folding entropy. How does the introduction of chirality affect the distribution of conformations and the entropy of folding? We first calculate the distributions of conformations over compactness ρ for a given main chain length N . The fraction $f(\rho)$ of conformations with compactness ρ is:

$$f(\rho) \equiv \frac{\omega(\rho)}{\sum_{\rho} \omega(\rho)},$$

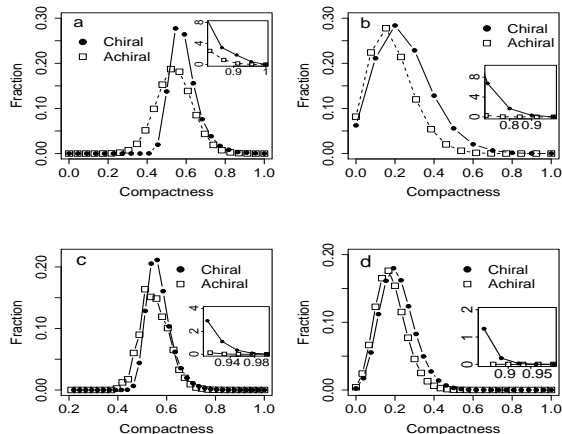


FIG. 7: Distribution of conformations over compactness for models of side chain size one (a) polymer chains of length 16 on two-dimensional square lattice (2Za1 and 2Zc1) obtained by exhaustive enumeration, (b) polymer chains of length 16 on three-dimensional tetrahedral lattice (3Ta1 and 3Tc1) obtained by exhaustive enumeration, (c) polymer chains of length 30 on two-dimensional square lattice obtained by sequential Monte Carlo, and (d) polymer chains of length 30 on three-dimensional tetrahedral lattice obtained by sequential Monte Carlo.

where $\omega(\rho)$ is the number of conformations found with compactness ρ .

The distributions of enumerated conformations of chiral and achiral polymers at length 16 on two-dimensional square lattice and three-dimensional tetrahedral lattice are shown in Figures 7a and 7b, respectively. The distribution of conformations at length 30 estimated by sequential Monte Carlo for both square and tetrahedral lattice are shown in Figures 7c and 7d, respectively. The inserts provide details of conformations in compact region. Distributions of less compact conformations may be useful for modeling proteins in unfolded state. Results from enumeration and sampling show similar patterns. In both two and three dimensional space, chiral and achiral polymers have low average compactness when the only interaction between residues is due to excluded volume, as in good solvent. However, the distributions of conformations of these two chirality models are clearly different. Chiral models have overall more compact conformations than achiral models.

Since proteins are highly compact, we consider conformations in high compactness region, especially in the region where $\rho = 1$. We calculate the folding entropy ΔS_f for the ensemble of conformations with

TABLE I: Number of conformations of a n -polymer by enumeration for different side-chain models. Here “2Z” stands for two-dimensional square lattice, “3T” for three-dimensional cubic lattice, “c” for chiral models, “a” for achiral models, “1” and “2” for side-chain models of 1 and 2 atoms, respectively, “M1–M3” for specific models of side-chain flexibility, where the second side chain atom can have 1–3 allowed positions, respectively. Specifically, we have: 2Za1: square lattice achiral model with side chain size of one, 2Zc1: square lattice chiral model with side chain size of one, 3Ta1: tetrahedral lattice achiral model with side chain size of one, 3Tc1: tetrahedral lattice chiral model with side chain size of one, 3Tc2.M1–M3: tetrahedral lattice chiral model with side chain size of two and flexibility models of M1–M3, respectively.

n	2Za1	2Zc1	3Ta1	3Tc1	3Tc2.M1	3Tc2.M2	3Tc2.M3
3	6	3	2	1	1	2	3
4	36	9	12	3	3	12	27
5	152	19	72	9	9	70	237
6	688	43	432	27	25	377	1888
7	2784	86	2336	73	63	1820	13659
8	11744	182	12992	203	158	8784	98202
9	47488	360	70720	553	386	41002	692820
10	195872	740	388096	1519	931	189167	4833081
11	791552	1453	2095872	4109	2220	859214	33447567
12	3233568	2930	11392416	11179	5309	3913808	231456640
13	13046720	5698	61468544	30240	12695	17752390	1596526404
14	53015776	11343	332851456	82021	30281	80385077	11002320270
15	213565776	21847	1792133312	221401	72159	363404876	75735208118
16	864828096	43072	9674958976	598996	171914	1642367812	NA
17	3478827632	82297	52031751936	1614693	409056	7413318612	NA
18	14051949392	160938	280368151936	4360282	972797	33449593868	NA
19	NA	305280	NA	11741404	2311751	NA	NA
20	NA	592686	NA	31661162	5491818	NA	NA

maximum compactness $\rho = 1$ and entropic change $\Delta S(\rho)$ at other compactness region. Figures 8a and 8b show exact ΔS_f and $\Delta S(\rho)$ for two and three dimensional polymers of length 16 calculated by enumeration.

For chiral models, the change in entropy during folding to conformations of maximum compactness is much smaller than that of achiral models. For chiral and achiral conformations on tetrahedral lattice with side chain size 1 (3Tc1 and 3Ta1 in Table I), the fraction of maximum compact conformations is much higher for chiral molecules (1.8×10^{-5}) than for achiral molecules (4.96×10^{-9}) at length 16. Chirality clearly favors compact conformations, despite the fact that the absolute number of conformations of maximum compactness is much smaller for chiral model (11 conformations) than for achiral models (144 conformations).

k. Excess folding entropy due to chirality. To examine the differences of folding entropy for polymers under two different chirality models, we calculate excess entropy of folding $ES_{c,a}(\rho)$ of chiral

model over achiral model for conformations at maximum compactness $\rho = 1.0$. The scaling relationships of $ES_{c,a}(1.0)$ with polymer backbone length N are shown in Figures 9a and 9b for square lattice model and tetrahedral lattice model, respectively. It provides information on whether and how the effects of chirality changes with chain length.

Exact $ES_{c,a}(1.0)$ obtained by enumeration in square lattice up to $N = 18$ fluctuates with chain length (Figure 9a, unfilled circles). In tetrahedral lattice, $ES_{c,a}$ increases with N to 8.2 at length $N = 16$ (Figure 9b, unfilled circles). This trend becomes clearer in results obtained by sequential Monte Carlo for conformations up to length $N = 50$ (Figure 9b). When chain length increases, the excess entropy increases linearly. This suggests that the effect of chirality on entropy of folding increases with chain length in tetrahedral lattice. For tetrahedral lattice, this relationship can be characterized by a linear regression ($R^2 = 0.98$) with $ES_{c,a}(1.0, N) = aN + b$, with $a = 0.75 \pm 0.06$, $b = -4.7 \pm 2.4$. The effects of chirality in increasing the fraction of compact chains

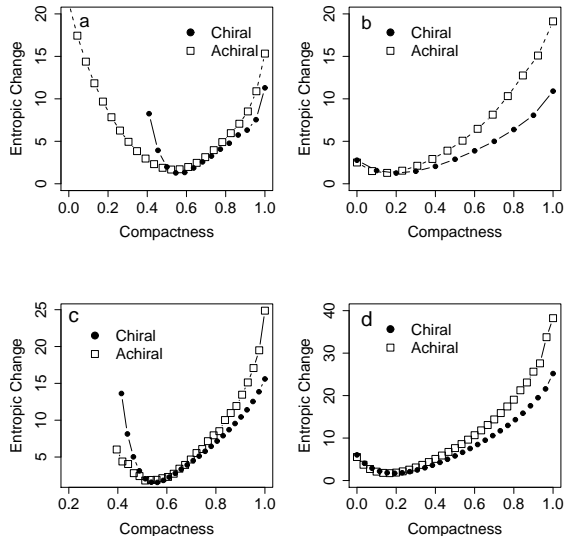


FIG. 8: Folding entropy for different models of chirality with side chain size of one. (a) Exact folding entropy ΔS_f at maximum compactness and entropic change $\Delta S(\rho)$ at other compactness regions ρ for polymers of length 16 calculated by exhaustive enumeration on two-dimensional square lattice, (b) Exact folding entropy ΔS_f and entropic change $\Delta S(\rho)$ for polymers of length 16 calculated by exhaustive enumeration on three-dimensional tetrahedral lattice, (c) Estimated ΔS_f and $\Delta S(\rho)$ for polymers of length 30 calculated by sequential Monte Carlo on two-dimensional square lattice. and (d) on three-dimensional tetrahedral lattice.

become more pronounced as chain length increases. In square lattice the effect of chirality to excess folding entropy also increases with chain length, but the trend is not as clear as that in tetrahedral lattice.

C. Effects of side chain flexibility

Because natural amino acid residues are three dimensional chiral molecules, we describe only results on flexibility effects using chiral models on three-dimensional tetrahedral lattice. A benefit from studying chiral model is that the conformational space of side chain is greatly reduced, and the folding entropy can be studied for longer polymers. We omit results on two dimensional square lattice, which are similar to that of tetrahedral lattice shown here.

l. Distribution of conformations and folding entropy. To study the effect of side chain flexibility, we first examine the exact distributions of conformations

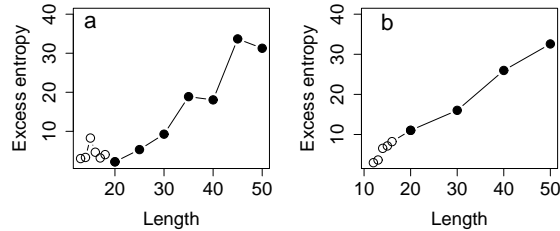


FIG. 9: Excess folding entropy due to chirality for maximum compact conformations calculated for models of side chain size one, (a) on two-dimensional square lattice, and (b) on three-dimensional tetrahedral lattice. Unfilled circles are excess folding entropy calculated by exact enumeration. Filled circles are excess folding entropy estimated by sequential Monte Carlo.

mations obtained by enumeration for polymers of length $N = 12$. These are obtained for three different models M_1, M_2 , and M_3 of different side chain flexibility, where the second side-chain atom can have 1, 2, and 3 allowed positions, respectively. The distributions of conformations of the three models show that M_1 has much higher average compactness compared to the other two models (Figure 10a). That is, less flexible side chains are more likely to form compact conformations. M_1 model also has the lowest folding entropy for compact conformations (Figure 10b). Model M_2 and M_3 have similar distribution, with M_2 slightly more compact on average.

For polymers of chain length $N = 30$, the distributions of conformations estimated by sequential Monte Carlo show a similar pattern. Conformations from model M_1 on average are more compact (Figure 10c): the largest number of conformations are found around $\rho \approx 0.42$ compared to $\rho \approx 0.34$ for model M_2 and model M_3 . For compact conformations (*e.g.*, $\rho \geq 0.8$), the entropic change is also much smaller for M_1 model of inflexible side chains. This suggests that there is a significant decrease in folding entropy when side chain loses its flexibilities.

m. Excess folding entropy due to side chain flexibility. The excess entropy of folding $E_{M_1, M_3}(1.0)$ of model M_1 compared to model M_3 for maximum compact conformations is shown in Fig 11. It can be characterized by a linear regression $E_{M_1, M_3}(1.0, N) = aN + b$, with $a = 0.27 \pm 0.03$, $b = 4.75 \pm 1.0$, and $R^2 = 0.90$. These results suggest that inflexibility of side chain plays an important role for obtaining compact conformations. The effects of inflexibility in increasing the fraction of

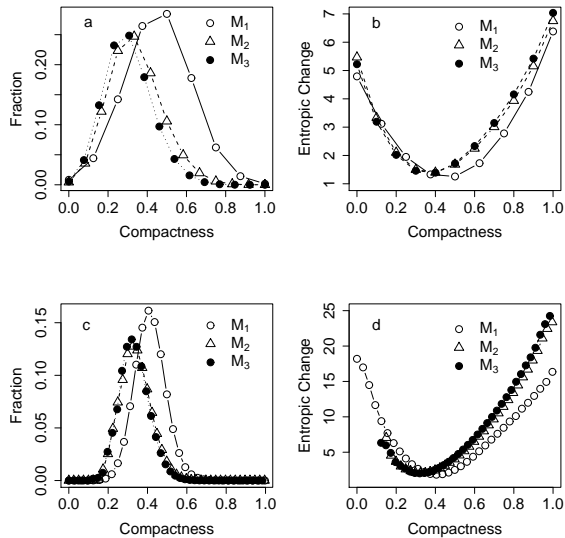


FIG. 10: Distribution of conformations and folding entropy over compactness for models with different side chain flexibility. Exact distribution of (a) conformations and (b) folding entropy for chains of length 12 obtained by exhaustive enumeration, and estimated distribution of conformations (c) and folding entropy (d) for chains of length 30 obtained by sampling.

compact chains become more pronounced as chain length increases.

D. Effects of side chains: packing, entropy, and secondary structure.

n. Jigsaw puzzle or nuts and bolts? Two differing views on the effects of side chains can be summarized by the model of jigsaw puzzle and the model of nuts and bolts (Fig 12). This comparison was studied in details in the seminal work of reference¹, where homopolymers of side chain of size one are studied. According to the nuts and bolts model, a small expansion in the volume of compact native protein leads to a large increase in side-chain entropy. That is, side-chain entropy increases sharply as main chain becomes less packed than native state. According to the jigsaw puzzle model, a small expansion in volume does not lead to significant change in side chain entropy when the molecule is compact. In a model supporting the jigsaw puzzle mode, it is estimated that a 25% expansion in volume relative to the native core volume is required before a sudden unfreezing of core side-chain rotameric de-

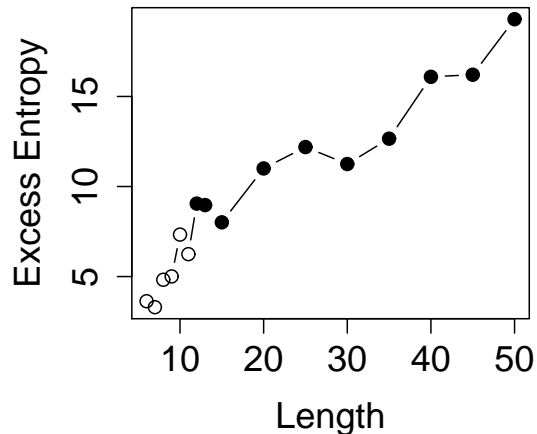


FIG. 11: Excess entropy of folding for conformations from M_3 model over conformations from M_1 model estimated by sequential Monte Carlo.

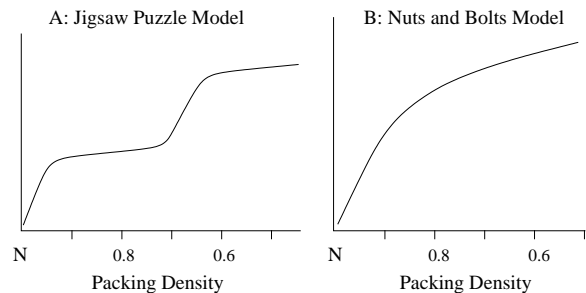


FIG. 12: A schematic comparison shows the qualitative difference in the dependencies of side-chain entropy on chain density in (a) a jigsaw puzzle model for side-chain packing, in which a side chain freezing effect occurs at near compact region; and (b) a nuts and bolts model in which main chain and side chain degrees of freedom are linked. (Adapted from Fig 13 in¹)

grees of freedom incurs a sharp increase in entropy³⁵. In a model supporting the nuts and bolts model, a small expansion in volume from the compact native state produces a steep increase in side-chain rotational entropy¹. The increase in side-chain degrees of freedom is linked to the increase in main-chain degrees of freedom¹. In this study, the size of the side chain is 1. For real proteins, except glycine and alanine, all other amino acid residues have more than one heavy atom in their side chains. What effects do side chains of larger sizes have on side chain packing? With the method of exact computation of side chain

entropy, we revisit this problem and examine the packing of chiral polymers with side chains formed by two atoms (M_3 model). Following reference¹, we use the radius of gyration R_g of backbone monomers to measure main chain packing density.

We examine the distribution of side chain entropy S_{sc} over the full range of main chain packing density measured by R_g . Exact calculation of side chain entropy for each of the exhaustively enumerated main chain conformation of length 10 shows that side chain entropy does not always correlate well with main chain packing density (Figure 13a). Conformations with most extended main chain structures ($R_g = 2.2 - 2.4$) are not those with maximum side chain entropy, and many compact conformations ($R_g \approx 1.4$) have very large side chain entropy.

We then use sequential Monte Carlo to generate longer main chain structures up to length 30, and calculate exactly the side chain entropy for each of the sampled main chain structures. We assess the correlation of side chain entropy and main chain backbone packing by calculating the average side chain entropy for conformations whose backbone R_g value falls into different intervals. As shown in Figure 13b, although some of the compact main chain structures of length 30 have very small R_g , they can still have substantial side chain entropy.

On average, there is a sharp decrease in the number of side chain conformations at compact regions where main chain R_g values are small for polymers of chain length $N = 20$. There is no plateau at compact regions with small R_g value, which would be characteristic of the jigsaw puzzle model. Our study using chiral model of homopolymers with two side chain atoms therefore is consistent with the nuts and bolts model of protein packing.

o. Rotamer counting. Estimating side chain entropy is an important problem that received much attention^{19,20,36,37}. For example, it was proposed in ref.³⁷ that side-chain entropy should be used as a criterion alternative to packing density to assess protein packing. Models developed in this study allow us to calculate explicitly side-chain entropy. We compare the numbers of side chain conformations obtained by exact calculation and by estimation using rotamer counting. With sequential Monte Carlo, we can access polymers in the full range of main chain compactness, including both maximum compact backbones and fully extended backbones, as well as polymers with compactness in-between. Because each sampled conformation is properly weighted, we have thus an accurate picture of the full distribution of all feasible geometric con-

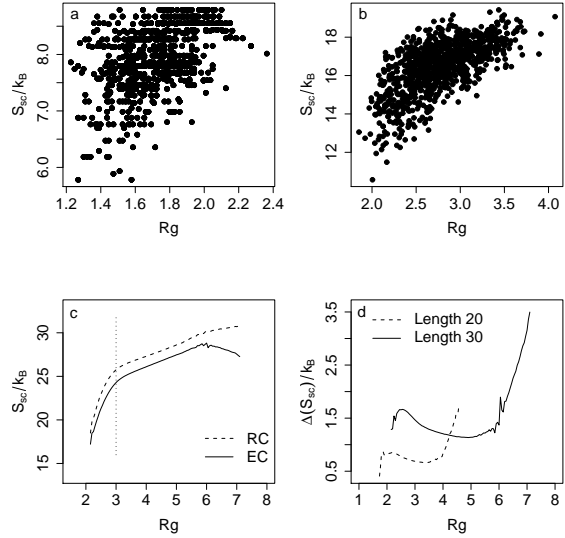


FIG. 13: Side chain entropy and main chain compactness of tetrahedral chiral conformations with two-atom side chains, where the second atom can have three allowed positions. (a) Exact number of side chain conformations for all main chain structures of length 10 over the main chain radius of gyration (R_g), (b) Exact number of side chain conformations for a set of 1,000 samples of main chain structures of length 20 over R_g , c) Expected side chain entropies of main chain structures of length 30 at different radius gyration, as estimated from exact calculation of side chain entropy based on 1,000,000 properly weighted samples of main chain structures (EC, solid line). Resampling technique described in³² was used to obtain samples in each intervals of R_g values. For comparison, side chain entropies estimated by rotamer counting are also plotted (RC, dotted line), and (d) Difference in expected side chain entropy by exact calculation and rotamer counting from sampled backbone structures at length 20 (solid line) and 30 (dotted line).

formations for various side chain models. This is different from other approaches such as molecular dynamics, where one typically samples conformations around the native structure³⁸.

We find that the number of side chain conformation by rotamer counting is consistently higher than the number obtained from exact enumeration (Figure 13c and 13d). The difference between these two methods varies at different main chain compactness. Over-estimation by rotamer counting is especially large for very extended conformations. It is also pronounced near the maximum compact region. That is, there is substantial unaccounted effect of side chain correlation in reducing side chain entropy due

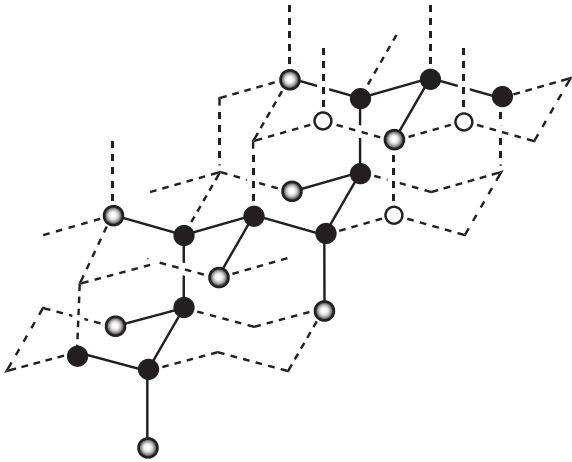


FIG. 14: Side chain entropy and compactness constraint favor the formation of helix-like structures. An example of main chain structure of length 10 with maximum side chain entropy is shown here. It adopts a helix-like conformation.

to excluded volume for rotamer counting, and this effect is more pronounced in both extended and near maximum compact regions.

p. Side chain entropy, compactness, and secondary structures. How does side chain entropy affect the formation of secondary structures? An example of a conformation at length $N = 10$ from tetrahedral chiral M_3 model (two side chain atoms with three possible position for the second atom) with maximum number of possible side chain conformations is shown in Figure 14. Since the second side chain atom in M_3 model can have three possible sites, side chain entropies of different residues may be correlated due to excluded volume effect if their side chain atoms can reach the same lattice site. The backbone structure of this particular conformation is arranged in such a way that none of the second atoms from different side chains can occupy the same lattice site. That is, in the conflict graph of this backbone, all vertices representing individual residues are disconnected, and there are $N = 8$ independent components in the graph. There is no correlation between side chain entropies of any residues in this backbone structure, and the total side chain entropy is simply determined by the total number of states of side chain $\prod_{i=1}^N n_i$, where $n_i = 3$ for M_3 model. It is remarkable that the spatial arrangement of this backbone structure resembles that of a helix. This suggests that the formation of helical secondary structures is strongly favored by side chain entropy for compact conformations.

In contrast, the most extended backbone has

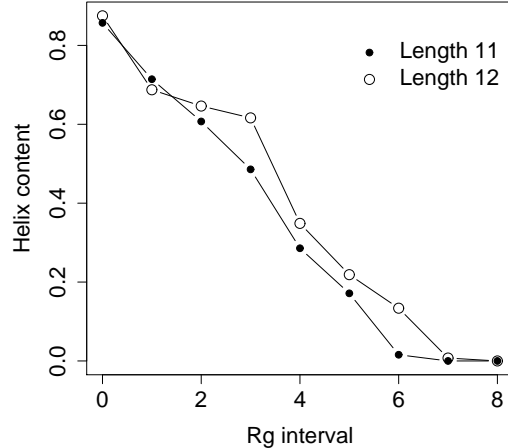


FIG. 15: Distributions of mean helix content for backbone conformations of M_3 model with maximum side chain entropy at different compactness for chains of length $N = 11$ and $N = 12$ as measured by radius of gyration R_g . We use 9 bins of uniform width for backbone conformations whose R_g values are all within the range of 1.8 to 2.4 lattice unit length. Compact backbone conformations have higher helix content (*e.g.*, the 0-th and the 1-st bins).

much smaller side chain entropy (Figure 5). Although the second atom of all side chain can have three possible positions, an empty site reachable from two residues can be taken by the side chain of only one residue, and the total number of possible states for side chains is much smaller. The conflict graph of the backbone structure in Figure 5 has only two independent disconnected components, one formed by residues whose side chains are pointing up, and another formed by those whose side chains are pointing down. We found that the mean helix content for backbones with maximum side chain entropy increases rapidly as backbones become more compact. Intra-chain hydrogen bond has long been thought as the determining factor for the formation of helical secondary structures. Side chain entropy was shown as an opposing factor for helix formation by molecular dynamics simulation³⁹. Results obtained here show that the combination of side chain entropy and compactness constraint lead to preference of helix formation (Figure 15). Helices have been observed in polyproline molecules as small as three to five residues on the basis of vibrational and ultraviolet CD measurements⁴⁰. Polyproline molecules cannot form intrachain hydrogen bond. Experimental results on polypeptoids also suggest

that side chain entropy can lead to formation of significant helical structures⁴¹. For example, artificially synthesized polypeptoids lack amide protons and are incapable of forming intra-chain hydrogen bonds. However, they can form monomeric alpha helices, as evidenced by CD spectra studies of pentameric and octameric peptoids. These alpha helices display characteristics of peptide behavior such as cooperative pH- and temperature-induced unfolding in aqueous solution. Examination of the structural details of these artificially synthesized polypeptoids indicates that side chain steric interaction in extended conformations of backbone is effectively avoided in helical conformations, as shown in our model study. Excluded volume effect of side chains leads to preference of helical backbone conformations over extended backbone conformations. This consideration may be useful for rational design of foldable polymer.

IV. DISCUSSION

In this study, we have developed two and three dimensional lattice models with explicit side chains. We make the distinction between the effects due to side chain chirality and to side chain flexibility. Side chains do not readily convert between configurations of different chiralities, whereas flexible side chains with two or more atoms can easily take different rotameric states when spatially feasible. We examine specifically the effects of side chain chirality and side chain flexibility on the distribution of polymers at different compactness, and their effects on folding entropy.

We find that polymers from chiral models on average are more compact than those from achiral models. Chiral models also have significantly smaller folding entropy into compact conformations than achiral models. The excess folding entropy between achiral models and chiral models increase linearly with chain length for long chains, suggesting the effects of chirality becomes more important for long chain polymers.

We also find that models with less flexible side chains have lower entropy of folding than those with more flexible side chains. Polymers with more flexible side chains may be thought to have better chance to fit into a compact state. However, there is a large entropic cost associated with flexible side chains. The excess entropy of flexible over inflexible side chain models also increases with chain length. These findings suggest that amino acid residues in proteins

need to maintain a reduced flexibility to ensure fast folding and stable native structure.

With explicit side chains, our study also confirms the conclusion of an earlier study based on simpler side chain models, namely, side chain packing is more like nuts-and-bolts rather than jigsaw puzzle, and main chain and side chain degrees of freedom are linked.

It is informative to examine the side chain flexibility of natural amino acid residues. Among the 20 amino acids, all non-polar amino acid residues either have branched side chains, or are aromatic with ring structures. On average they are rather inflexible. The total number of rotatable bonds divided by the number of side chain atoms is small (Table II). In contrast, side chains of polar or ionizable residues such as lysine and arginine have more rotatable bonds and have higher flexibilities. However, this difference can be rationalized by the observation that side chains of polar and ionizable residues often are involved in electrostatic ion pair interactions or hydrogen bonding interactions when buried in protein interior, hence they have effectively reduced flexibility. The overall flexibilities of side chains of all natural residues are therefore relatively small. This reduced flexibility may be necessary to decrease the entropy opposing folding to compact state.

Examination of patterns of side chain rotamer libraries further confirms this observation. We use a parameter f for the number of rotamers per atom defined as $f = n_r/n_a$, where n_r is the number of all possible rotamers for a specific side chain type and n_a is the number of heavy atoms in that side chain type. By the criterion of hydrophobicity⁴², we divide twenty amino acids into three categories: hydrophilic residues (hydrophobicity < 0.3), hydrophobic residues (hydrophobicity > 0.75), and neutral residues ($0.3 \geq \text{hydrophobicity} \leq 0.75$). According to this division, there are seven hydrophobic residue types, seven hydrophilic residue types, and six neutral residue types.

We calculate the weighted expected number of rotamers per atom \bar{f} for each residue group, where the weighting factor is taken as the frequency of occurrence of the specific amino acid residue type in eukaryotic proteins (see ref.⁴³). The number of possible rotamers for each residue type is taken from reference⁴⁴. The expected \bar{f} values are 1.10, 1.34, and 2.74 for hydrophobic, neutral, and polar amino acid residues, respectively. Polar residues have the largest \bar{f} value, but they are frequently involved in electrostatic interactions and hydrogen bonding, which significantly decreases the actual flexibility of

TABLE II: Side chain flexibility of naturally occurring amino acid residues. H: hydrophobic residues, P: hydrophilic or polar residues, N: neutral residues, $f = N_r/N_a$: number of rotamers per atom. Values in parenthesis after residue names are hydrophobicity values of amino acid residues as given in⁴², and values in parenthesis after $f = N_r/N_a$ values are the relative frequency of occurrence of the corresponding amino acid residue in percentage⁴³.

H	N_r/N_a	N	N_r/N_a	P	N_r/N_a
F(1.0)	0.57(4.29)	A(0.62)	1.00(6.24)	D(0.028)	1.25(5.38)
I(0.94)	1.75(5.80)	C(0.68)	1.50(1.70)	E(0.043)	1.60(6.57)
L(0.94)	1.25(9.40)	G(0.50)	-(5.64)	H(0.165)	1.33(2.33)
V(0.83)	1.00(5.99)	M(0.74)	3.25(2.21)	K(0.283)	5.40(6.46)
W(0.87)	0.70(1.11)	P(0.71)	1.00(4.96)	N(0.236)	1.75(5.08)
Y(0.88)	0.50(3.15)	S(0.36)	1.50(8.67)	Q(0.251)	1.80(4.23)
		T(0.45)	1.00(5.60)	R(0.000)	4.86(4.99)
Average	1.10(29.74)		1.34(35.02)		2.74(35.04)

polar side chains. In general, \bar{f} values for natural amino acid residues are small, indicating that by the criterion of weighted number of rotameric states per side chain atom, they are rather inflexible.

It is remarkable that helix emerges as preferred main chain structure for compact main chain conformations with maximum side chain entropy. Our results indicate that the correlation between side chains plays significant role in protein entropy and should be modeled more accurately. Real proteins have far more complex side chains. For example, to model a Lys residue realistically, a model of side chain of size 5 with all connecting flexible bonds is needed. The associated side chain conformational space is much larger than the M_3 model developed in this study, and therefore is not amenable to detailed analysis. However, we believe the conclusion obtained using M_3 model that inflexible side chain reduces folding entropy remains valid if longer and more flexible side chain model is used. In real proteins, there are many residues whose side chains have flexibility comparable to that of M_3 model (*e.g.*, His, Phe, Tyr, Val, Ser, Cys, if we regard the inflexible part of their side chains as one side chain bead in the M_3 model). For these residues with reduced side chain flexibility, we find that side chain entropy promotes the formation of helix for compact main chain conformations.

Estimating side chain entropy is an important and difficult task for modeling protein structure and protein stability. With explicit side chain models on three dimensional tetrahedral lattice, we have developed an algorithm that calculates the exact side chain entropy of tetrahedral lattice models for any given main chain structures of moderate length.

With current implementation, it works well up to chain length of 30. We compare results of side chain entropy calculated by rotamer counting and by the exact method developed here. For longer chain polymers (*e.g.*, $N = 30$), we found rotamer counting method can give significantly over-estimated side chain entropy. For example, the average difference between the two methods for models of length $N = 30$ is larger for extended main chain structures ($R_g > 6.5$) and near compact main chain structures ($R_g = 2.7 - 2.9$, Figure 13d).

The method for exact calculation of side chain entropy given a backbone structure can be generalized. For longer chains, each disconnected component in the conflict graph could contain too many residues such that enumeration becomes infeasible. It is possible to further develop an algorithm using the same divide-and-conquer approach, where the large independent component is decomposed further into two roughly equal size disconnected components by removing a small number of edges in the conflict graph. As an illustration, the larger independent component in Figure 5 formed by monomer 1, 3, 5, and 7 can be decomposed into two small disconnected components by cutting the edge between vertices 4 and 6, which corresponds to the shared position (labeled as “a”). The two smaller components can then be enumerated separately, and side chains of residues connected by the cut edges can also be enumerated individually. These enumeration will provide an exact value for the total possible side chain arrangements of the original larger independent component. When a disconnected components contain a large number of residues, an optimal decomposition becomes difficult. This is related to the graph par-

tition problem. Although finding an optimal solution to this problem is known to be an NP-complete problem⁴⁵, there are many effective approximation and heuristic algorithms that are applicable for obtaining a good decomposition.

Side chains in natural amino acid residues are chiral, and proteins are better characterized using chiral models. Chiral models developed in this study will be useful for exploration of other properties of proteins, where side chains play important roles. Achiral models introduced here may also be useful to study other polymers with transient chirality on backbone⁴⁶, or branched polymers such as peptoids,

in which the chirality on nitrogen atom is unstable and the side chain can easily convert between opposite configuration⁴¹.

V. ACKNOWLEDGMENT

We thank Dr. Clare Woodward for helpful discussions. This work is supported by grants from National Science Foundation (CAREER DBI013356, DBI0078270, DMC0073601, CCR9980599), and National Institute of Health (GM68958).

-
- ¹ S. Bromberg and K.A. Dill. Side chain entropy and packing in proteins. *Protein Sci*, 3(7):997–1009, 1994.
- ² A.D. Miranker and C.M. Dobson. Collapse and cooperativity in protein folding. *Curr. Op. Struct. Biol.*, 6(1):31–42, 2 1996.
- ³ R. Wynn, P.C. Harkins, F.M. Richards, and R.O. Fox. Mobile unnatural amino acid side chains in the core of staphylococcal nuclease. *Protein Science*, 5(6):1026–1031, 6 1996.
- ⁴ J.B.O. Mitchell, R.A. Laskowski, and J.M. Thornton. Non-randomness in side-chain packing: The distribution of interplanar angles. *Proteins*, 29(3):370–380, 11 1997.
- ⁵ D.K. Klimov and D. Thirumalai. Cooperativity in protein folding: from lattice models with sidechains to real proteins. *Fold & Des*, 3(2):127–139, 1998.
- ⁶ F.M. Richards and W.A. Lim. An analysis of packing in the protein folding problem. *Q. Rev. Biophys.*, 26:423–498, 1994.
- ⁷ J. Liang and K.A. Dill. Are proteins well-packed? *Biophys. J.*, 81(2):751–766, 2001.
- ⁸ Z. Bagci, R.L. Jernigan, and I. Bahar. Residue packing in proteins: Uniform distribution on a coarse-grained scale. *J. Chem. Phys.*, 116:2269–2276, 2002.
- ⁹ K.A. Dill, S. Bromberg, K. Yue, K.M. Fiebig, D.P. Yee, P.D. Thomas, and H.S. Chan. Principles of protein-folding - a perspective from simple exact models. *Protein Science*, 4(4):561–602, 4 1995.
- ¹⁰ E. Kussell and E.I. Shakhnovich. Glassy dynamics of side-chain ordering in a simple model of protein folding. *Phys. Rev. Lett.*, 89:168101, 2002.
- ¹¹ C. Micheletti, J. Banavar, A. Maritan, and F. Seno. Steric constraints in model proteins. *Phys. Rev. Lett.*, 80:5683–5686, 1998.
- ¹² R.L. Dunbrack and M. Karplus. Conformational-analysis of the back-bone-dependent rotamer preferences of protein side-chains. *Nat Struct Biol*, 1:334–340, 1994.
- ¹³ E.L. Eliel and S.H. Wilen. *Stereochemistry of organic compounds*. Wiley, New York, 1994.
- ¹⁴ J.R. Cronin, S. Pizzarello, and D.P. Cruikshank. *Meteorites and the early Solar System*. University of Arizona Press, 1988.
- ¹⁵ J.R. Cronin and S. Pizzarello. Amino acids in meteorites. *Adv. Space Res.*, 3:5–18, 1983.
- ¹⁶ F.M. Richards. Protein stability: still an unsolved problem. *CMLS. Cell. mol. life sci.*, 53:790–802, 1997.
- ¹⁷ R. L. Dunbrack Jr. Rotamer libraries in the 21st century. *Curr. Op. Struct. Biol.*, 12:431–440, 2002.
- ¹⁸ E. Kussell, Shimada J., and Shakhnovich E.I. Excluded volume in protein side-chain packing. *J. Mol. Biol.*, 311(1):183–193, 2001.
- ¹⁹ G.P. Brady and K.A. Sharp. Entropy in protein folding and in protein-protein interactions. *Curr. Op. Struct. Biol.*, 7(2):215–221, 1997.
- ²⁰ A.J. Doig and M.J.E. Sternberg. Side-chain conformational entropy in protein folding. *Protein Science*, 4(11):2247–2251, 1995.
- ²¹ C. Cole and J. Warwicker. Side-chain conformational entropy at protein-protein interfaces. *Protein Science*, 11(12):2860–2870, 12 2002.
- ²² S.D. Pickett and M.J.E. Sternberg. Empirical scale of side chain conformational entropy in protein folding. *J Mol Biol*, 231:825–839, 1993.
- ²³ B.H. Park and M. Levitt. The complexity and accuracy of discrete state models of protein structure. *J Mol Biol*, 249:493–507, 1995.
- ²⁴ Y. Xia, E.S. Huang, M. Levitt, and R. Samudrala. Ab initio construction of protein tertiary structures using a hierarchical approach. *J Mol Biol*, 300:171–185, 2000.
- ²⁵ E. Flapan. *When Topology Meets Chemistry : A Topological Look at Molecular Chirality*. Cambridge University Press, 2000.
- ²⁶ R.L. Dunbrack and F.E. Cohen. Bayesian statistical analysis of protein side-chain rotamer preferences. *Protein Science*, 6(8):1661–1681, 8 1997.
- ²⁷ K.F. Lau and K.A. Dill. A lattice statistical mechanics model of the conformational and sequence spaces of proteins. *Macromolecule*, 93:6737–6743, 1989.
- ²⁸ R.I. Dima and D. Thirumalai. Asymmetry in the shapes of folded and denatured states of proteins.

- arXiv*, 1:q-bio.BM/0310023, 2003.
- ²⁹ J. Zhang, R. Chen, C. Tang, and J. Liang. Origin of scaling behavior of protein packing density: A sequential Monte Carlo study of compact long chain polymers. *J. Chem. Phys.*, 118:6102–6109, 2003.
- ³⁰ J.S. Liu and R. Chen. Sequential monte carlo methods for dynamic systems. *Journal of the American Statistical Association*, 93:1032–1044, 1998.
- ³¹ Jun S. Liu. *Monte Carlo strategies in scientific computing*. Springer, New York, 2001.
- ³² J. Liang, J. Zhang, and R. Chen. Statistical geometry of packing defects of lattice chain polymer from enumeration and sequential Monte Carlo method. *J. Chem. Phys.*, 117:3511–3521, 2002.
- ³³ H.S. Chan and K.A. Dill. Compact polymers. *Macromolecules*, 22:4559–4573, 1989.
- ³⁴ T.H. Cormen, C.E. Leiserson, and R.L. Rivest. *Introduction to algorithms*. The MIT Press, Cambridge, MA, 1990.
- ³⁵ E.I. Shakhnovich and A.V. Finkelstein. Theory of cooperative transitions in protein molecules I. why denaturation of globule protein is a 1st-order phase transition. *Biopolymers*, 28:1667–1680, 1989.
- ³⁶ T.P. Creamer. Side-chain conformational entropy in protein unfolded states. *Proteins*, 40(3):443–450, 8 2000.
- ³⁷ Y.B. Yu, P. Lavigne, P.L. Privalov, and R.S. Hodges. The measure of interior disorder in a folded protein and its contribution to stability. *J. Am. Chem. Soc.*, 121:8443–8449, 1999.
- ³⁸ H. Schafer, L.J. Smith, A.E. Mark, and W.F. van Gunsteren. Entropy calculations on the molten globule state of a protein: Side-chain entropies of alpha-lactalbumin. *Proteins*, 46(2):215–224, 2 2002.
- ³⁹ T.P. Creamer and G.D. Rose. Side-chain entropy opposes alpha-helix formation but rationalizes experimentally determined helix-forming propensities. *PNAS*, 89(13):5937–5941, 1992.
- ⁴⁰ R.K. Dukor and T.A. Keiderling. Reassessment of the random coil conformation. vibrational cd study of proline oligopeptides and related polypeptides. *Biopolymers*, 31:1747–1761, 1991.
- ⁴¹ K. Kirshenbaum, A.E. Barron, R.A. Goldsmith, P. Armand, E.K. Bradley, Truong K.T.V., K.A. Dill, F.E. Cohen, and R.N. Zuckermann. Sequence-specific polypeptoids: aa diverse family of heteropolymers with stable secondary structure. *Proc. Natl. Acad. Sci.*, 95:4303–4308, 4 1998.
- ⁴² S.D. Black and D.R. Mould. Development of hydrophobicity parameters to analyze proteins which bear post- or cotranslational modifications. *Anal. Biochem.*, 193:72–82, 1991.
- ⁴³ F. Tekaia, E. Yeramian, and B. Dujon. Amino acid composition of genomes, lifestyle of organisms and evolutionary trends : a global picture with correspondence analysis. *Gene*, 297:51–60, 2002.
- ⁴⁴ S.C. Lovell, J.M. Word, J.S. Richardson, and D.C. Richardson. The penultimate rotamer library. *Proteins*, 40:389–408, 2000.
- ⁴⁵ M.R. Garey and D.S. Johnson. *Computers and intractability: A guide to the theory of NP-completeness*. Freeman, 1979.
- ⁴⁶ D.J. Hill, M.J. Mio, R.B. Prince, T.S. Hughes, and J.S. Moore. A field guide to foldamers. *Chem. Rev.*, 101:3893–4011, 2001.